ISSN (Print) : 2320 – 3765
ISSN (Online): 2278 – 8875

International Journal of Advanced Research in Electrical, Electronics and Instrumentation Engineering

(An ISO 3297: 2007 Certified Organization)

Vol. 5, Issue 4, April 2016

Detection and Prediction of Lung Tumour Survival by Using SWFCM Clustering

R.Radhika[1], J.Anupriya[2], P.Elizabeth Mahilda[3], S.J.Jini Jerald[4]

Associate Professor, Dept. of ECE, S.A Engineering College, Chennai, India[1]

UG Student, Dept. of ECE, S.A Engineering College, Chennai, India[2]

UG Student, Dept. of ECE, S.A Engineering College, Chennai, India[3]

UG Student, Dept. of ECE, S.A Engineering College, Chennai, India[4]

ABSTRACT: In our daily life, Lung cancer seems to be the common cause of death among people throughout the world. Early detection of lung cancer can increase the chance of survival among people. The Computed Tomography (CT) can be more efficient than X-ray. However, problem seemed to merge due to time constraint in detecting the present of lung cancer regarding on the several diagnosing method used. Hence, a lung cancer detection system using image processing is used to classify the present of lung cancer in a CT- images. In this paper, MATLAB have been used through every procedures made. In image processing procedures, process such as image pre-processing, enhancement and segmentation have been discussed in detail. We are aiming to get the more accurate results by using various enhancement and segmentation techniques. This paper investigates spatially weighted fuzzy C-mean (SWFCM) techniques that allow detection of lung cancer.

KEYWORDS: CT lung image, SWFCM, image processing, segmentation

I.INTRODUCTION

Lung Cancer

Cancer is a group of diseases characterized by an abnormal and unregulated growth of cells. Tissue with abnormal cell growth is called a tumor and can be malignant or benign, which is the same as cancerous or non-cancerous.[1] The main differences are that a benign tumor grows slower, will not spread and will usually not come back if it is surgically removed. Lung cancer is, in competition with prostate and breast cancer, the most common type of cancer and the leading cause of death by cancer for both men and women in United States and Western Europe. The majority of all cases is caused by tobacco smoking. Exposure to asbestos, radon, uranium and arsenic are other risk factors. Lung cancer is a very deadly disease and has an inclination to metastasize (spread) to other parts of the body, e.g. the brain, liver, bone and bone marrow. In most cases this occurs before it is discovered. Usually, lung cancer happens after the age of 50.

There are two major groups of lung cancer, Small Cell Lung Cancer (SCLC) and Non-Small Cell Lung Cancer (NSCLC), which together cover more than 90% of all cases. They grow and spread in different ways and are treated differently. In general, SCLC, which is less common, is more aggressive and metastasizes faster. The methods for diagnosing lung cancer include CT scan (Computed Tomography), PET scan (Positron Emission Tomography), MRI (Magnetic Resonance Imaging), bronchoscopy (examination of the airways with fiber optics) and biopsy (examination of lung tissue sample). The last method can be used to decide the type of cancer depending on what the cancer cells look like in a microscope. The staging of lung cancer is an important step for deciding the right treatment. Currently, CT is used in the place of plain chest X-ray in detecting and diagnosing the lung cancer. The overall 5-year survival rate for lung cancer patients increases from 15 to 50% if the disease is detected in time.

ISSN (Print) : 2320 – 3765
ISSN (Online): 2278 – 8875

International Journal of Advanced Research in Electrical, Electronics and Instrumentation Engineering

(An ISO 3297: 2007 Certified Organization)

Vol. 5, Issue 4, April 2016

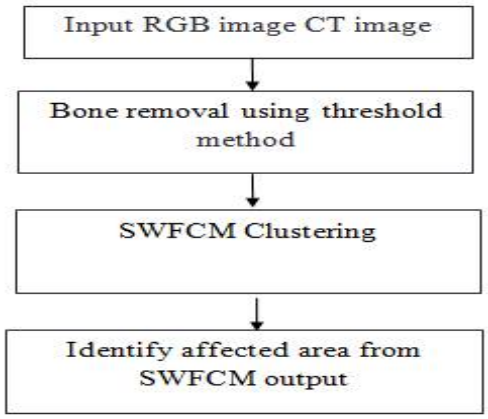

Figure 1: "Flow chart of the proposed method"

II. RELATED WORK

Abdullah3 stated that the segmentation of the lung region due to the limitation regarding on the similarities of the intensity in the x-ray image. As for lung cancer nodule detection process, it does not seem to be the problem because of the absent of the similar intensity due to the lung segmentation. It can be used in the lung in the lung cancer application and the system can also be used in the application such as the detection and classification of breast tumor in mammography images regarding on the higher variation of intensity present. Zare4 declared that the approaches of content-based image retrieval (CBIR) using low level features such as shape and texture are investigated in order to create a framework that classify medical x-ray image automatically. GLCM, canny edge operator, local binary pattern and pixel level information of the images act as image based feature representation.

The performance of image classification offered by combining the promising features stated above investigation. Experimental results using 116 different classes of 11,000 x-ray images 90.7% classification accuracy. Gomathi5 expressed that computer aided diagnosing system which uses FPMC algorithm for segmentation to improve the accuracy. Rule based technique is applied to classify the cancer nodule after segmentation. For its better classification, the learning is performed with the help of extreme learning machine. Jia Tong6 acknowledged that several steps are followed to detect the cancer like segmentation of lung parenchyma, the detection of suspicious nodule candidates, the feature extraction and classification. Here the author used adaptive threshold segmentation, math morphologic, Gaussian filter, Hessian matrix algorithms.

III.PROPOSED SYSTEM

CLUSTERING METHODS

Elimination of Bone Region

The bone region affects the segmentation accuracy so the first step is the removal of bone region from the lung CT image. Separate R-plane, G-plane, and B-plane from RGB Image.7 In this entire plane, the bone region is detected. Subtract all these images, so that the resultant image is T. T=R-G-B

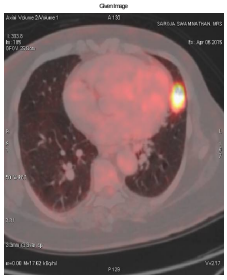

Figure 2 Input CT Image

ISSN (Print) : 2320 – 3765
ISSN (Online): 2278 – 8875

International Journal of Advanced Research in Electrical, Electronics and Instrumentation Engineering

(An ISO 3297: 2007 Certified Organization)

Vol. 5, Issue 4, April 2016

RGB (Truecolor) Images

An RGB image, sometimes referred to as a *truecolor* image, is stored as an *m*-by-*n*-by-3 data array that defines red, green, and blue color components for each individual pixel. RGB images do not use a palette. The color of each pixel is determined by the combination of the red, green, and blue intensities stored in each color plane at the pixel's location. Graphics file formats store RGB images as 24-bit images, where the red, green, and blue components are 8 bits each. This yields a potential of 16 million colors. The precision with which a real-life image can be replicated has led to the nickname "truecolor image."

An RGB MATLAB® array can be of class double, uint8, or uint16. In an RGB array of class double, each color component is a value between 0 and 1. A pixel whose color components are (0,0,0) is displayed as black, and a pixel whose color components are (1,1,1) is displayed as white. The three color components for each pixel are stored along the third dimension of the data array. For example, the red, green, and blue color components of the pixel (10,5) are stored in RGB(10,5,1), RGB(10,5,2), and RGB(10,5,3), respectively.

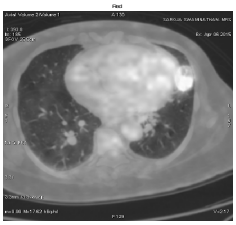

Figure 2 Red Plane

To display the truecolor image RGB, use the image function: image RGB). The next figure shows an RGB image of class double. Separate R-plane, G-plane, and B-plane from RGB Image. To determine the color of the pixel at (2,3), look at the RGB triplet stored in (2,3,1:3). Suppose (2,3,1) contains the value 0.5176, (2,3,2) contains 0.1608, and (2,3,3) contains0.0627. The color for the pixel at (2,3) is 0.5176 0.1608 0.0627.

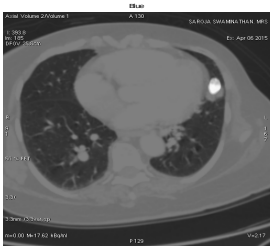

Figure 3 Blue plane

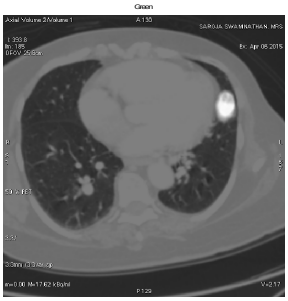

Figure 4 Green plane

ISSN (Print) : 2320 – 3765
ISSN (Online): 2278 – 8875

International Journal of Advanced Research in Electrical, Electronics and Instrumentation Engineering

(An ISO 3297: 2007 Certified Organization)

Vol. 5, Issue 4, April 2016

IV. SEGMENTATION

IMAGE ENHANCEMENT

Image enhancement processes consist of a collection of techniques that seek to improve the visual appearance of an image or to convert the image to a form better suited for analysis by a human or a machine. In general, there is no general unifying theory of image enhancement at present because there is no general standard of image quality that can serve as a design criterion for an image enhancement processor.

SEGMENTATION

In computer vision, **image segmentation** [5] is the process of partitioning a digital image into multiple segments (sets of pixels, also known as super pixels). The goal of segmentation is to simplify and/or change the representation of an image into something that is more meaningful and easier to analyze. Image segmentation is typically used to locate objects and boundaries (lines, curves, etc.) in images. More precisely, image segmentation is the process of assigning a label to every pixel in an image such that pixels with the same label share certain characteristics. In our project we used the Spatially Weighted Fuzzy c-means segmentation for segmentation purpose.

The FCM method is utilized by the previous researchers for fundus image segmentation. Though the quality of CT image will not be as good as the fundus image, SWFCM method is adopted for segmentation.

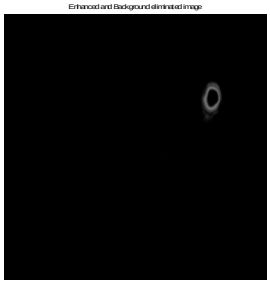

Figure 5 Enhance and bone removal image

V. ALGORITHM

SPATIALLY WEIGHTED FUZZY C-MEAN ALGORITHM

The standard FCM [6] does not consider the spatial information of pixels and in turn, the segmentation result is affected. One of the important characteristics of an image is that neighboring pixels are highly correlated which is considered in spatially weighted fuzzy C-mean (SWFCM) method. The FCM method is utilized by the previous researchers for image segmentation. [9]SWFCM method is adopted for corresponding region. The segmented image has three clusters, namely the backgrounds. The image with these three identified clusters (SWFCM output) is shown in the Figure 6.

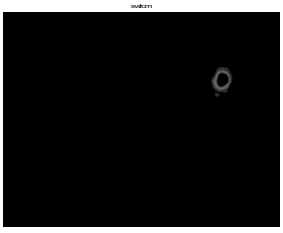

Figure 6 SWFCM output image

ISSN (Print) : 2320 – 3765
ISSN (Online): 2278 – 8875

International Journal of Advanced Research in Electrical, Electronics and Instrumentation Engineering

(An ISO 3297: 2007 Certified Organization)

Vol. 5, Issue 4, April 2016

Segmentation of Lung cancer Using SWFCM

SWFCM is applied to the images in which bones are already removed. One of the important characteristics of an image is that neighboring pixels are highly correlated. The spatial relationship is important in clustering, but it is not utilized in a standard FCM algorithm. In SWFCM, to exploit the spatial information, a spatial function is defined as

$$h_{ij} = \sum_{k \in NB(x_j)} u_{ik} \quad (1)$$

Where $NB(x_j)$ represents a square window centered on pixel x_j in spatial domain. Larger window size may blur the images and the smaller window size does not remove the noise at high density. Therefore, an optimal window of size 5x5 is used in this work. Just like the membership function, the spatial function h_{ij} represents the probability that the pixels x_j belong to the i[th]cluster. The spatial function of pixels is large if the majority of its neighborhood belongs to the same clusters. The spatial function is incorporated into membership function as follows

$$u'_{ij} = \frac{u_{ij}^{p} h_{ij}^{q}}{\sum_{k=1}^{c} u_{kj}^{p} h_{kj}^{q}} \quad (2)$$

Where P and Q are the controlling parameters. The spatial functions simply strengthen the original membership in a homogenous region, but it does not change clustering result. However, this formula reduces the weight of a noisy cluster in noisy pixels by the labels to its neighboring pixels.

The clustering is a two-pass process at each iteration. The first pass is the same as that in standard FCM to calculate the membership function. In the second pass, the membership information of each pixel is mapped to the spatial domain and the spatial domain function is computed from that. The FCM iteration proceeds with the new membership that is incorporated with spatial function. The iteration is stopped when the maximum difference between two cluster centers at two successive iterations is less than 0.00001. After the convergence, defuzzification is applied to assign each pixel to a specific cluster for which the membership is maximal.

SWFCM Algorithm

Generate the random number with the range from 0 to1 to be the initial memberships. Let us consider the number of cluster is N then calculate V_i using (3)

$$V_i = \frac{\sum_{j=1}^{N} u_{ij}^{m} x_j}{\sum_{j=1}^{N} u_{ij}^{m}} \quad (5)$$

Where,

V_i = i[th]cluster center

m = fuzziness parameter m=2

Where u_{ij} is by using Equation (3.21)

ISSN (Print) : 2320 – 3765
ISSN (Online): 2278 – 8875

International Journal of Advanced Research in Electrical, Electronics and Instrumentation Engineering

(An ISO 3297: 2007 Certified Organization)

Vol. 5, Issue 4, April 2016

$$u_{ij} = \frac{1}{\sum_{k=1}^{c} \left(\frac{\|x_j - v_i\|}{\|x_j - v_k\|} \right)^{2/(m-1)}} \quad (4)$$

Map u_{ij} into the pixel position and calculate the modified membership u'_{ij} using (6). Compute objective function J using (7)

$$J = \sum_{j=1}^{N} \sum_{i=1}^{c} u_{ij}^{m} \left| \|x_j - v_i\| \right|^2 \quad (5)$$

Update the cluster center using (5)

Repeat steps 2 to step 4 until the following termination criterion is satisfied:

$$\|J_{new} - J_{old}\| < \varepsilon \quad (6)$$

Whereε=0.00001 which is same as in the FCM method used previously in this work.From the detected affected area of the cancer. Figure 7 shows the superimposed original RGB image.

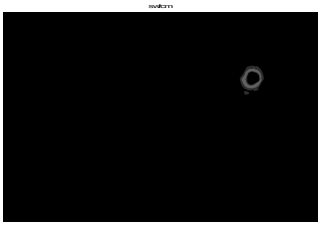

Figure 7 superimposed output image

VI. RESULTS AND DISCUSSIONS

Performance Parameters

The comparison of various classification algorithms is done on the basis of following performance parameters:

TP Rate: The True Positive (TP) rate is the proportion of examples which were classified as class x, among all examples which truly have class x, i.e. how much part of the class was captured. It is equivalent to Recall. In the confusion matrix, this is the diagonal element divided by the sum over the relevant row.

FP Rate: The False Positive (FP) rate is the proportion of examples which were classified as class x, but belong to a different class, among all examples which are not of class x. In the confusion matrix, this is the column sum of class x minus the diagonal element, divided by the rows sums of all other classes.

Where True positive TP= R n T; (7)
False Positive FP=R - (R n T); (8)
False Negative FN=T - (R n T). (9)

ISSN (Print) : 2320 – 3765
ISSN (Online): 2278 – 8875

International Journal of Advanced Research in Electrical, Electronics and Instrumentation Engineering

(An ISO 3297: 2007 Certified Organization)

Vol. 5, Issue 4, April 2016

A simple and effective overlap measure of the match between the ground truth region and detected. Region (R) by the proposed method is used to measure the accuracy (M) as follows:[8]

$$M = \frac{AREA(T \cap R)}{AREA(T \cup R)} \tag{10}$$

VII. CONCLUSION

Lung cancer is the most dangerous and widespread in the world according to stage the discovery of the cancer cells in the lungs, this gives us the indication that the process of detection this disease plays a very important and essential role to avoid serious stages and to reduce its percentage distribution in the world. In this approach, it is very simple to identify the stage and the affected tumor area in the lung tissue. i.e. CT scan images for the detection of Lung Nodule is cancerous or not. In this paper we show the potential of SWFCM segmentation is used.Besides its use as a potential screening tool for lung cancer, this method can be used to monitor treatment effectiveness, to detect the recurrence of lung cancer, and also to identify patients who may need an invasive diagnostic procedure. In future studies, we also plan to include larger study populations to establish statistical significance.

REFERENCES

[1] American Cancer Society (ACS), "Report on Lung Cancer," 2010
[2] Ada, Rajneet Kaur,"Feature Extraction and Principal Component Analysis for Lung Cancer Detection in CT scan Images",International Journal of Advanced Research in Computer Science and Software Engineering (IJARCSSE),Volume 3, Issue 3, March 2013
[3] Ali Nawaz Khanb, Hamdan AL-Jahdalia, Shukri Loutfic,Abdullah S. Al-Harbia "Guidelines for the role of FDG-PET/CT in lung cancermanagement", ELSEVIER Journal of Infection and Public Health Issue 5, pg.S35—S40,2012
[4] P.Nivetha, Mr.R.Manickavasagam "Lung Cancer Detection at Early Stage Using PET/CT Imaging Technique" Vol. 2, Issue 3, March 2014
[5] M.Gomathi and P. Thangaraj A Computer Aided Diagnosis System for Lung Cancer Detection \Using Support Vector Machine American Journal of Applied Sciences , 2010
[6] Gonzalez.RC & Woods.RE , 'Digital Image Processing', NJ. Prentice Hall, Second Edition,2005.
[7] Kavitha.D&Shenbaga Devi.S, 'Automatic detection of optic disc and exudates in retinal images', International Conference on Intelligent Sensing and Information Processing,2005 pp. 501-506.
[8] R. Shojaii, J. Alirezaie, and P. Babyn, "Automatic lung segmentation in CT images using watershed transform," in Proc. IEEE Int. Conf. Image Process., 2005, vol. 2, p. 270.
[9] L. Zhang, E. A. Hoffman, and J. M. Reinhardt, "Lung lobe segmentation by graph search with 3-D shape constraints," in Proc. SPIE, 2001, vol. 4321, pp. 204–215.
[10] P. Hua, Q. Song, M. Sonka, E. Hoffman, and J. Reinhardt, "Segmentation of pathological and diseased lung tissue in CT images using a graph search algorithm," in Proc. IEEE Int. Symp. Biomed. Imag: From Nano to Macro, 2011, pp. 2072–2075.
[11] T. N. Jones and D. N. Metaxas, "Automated 3-D segmentation using deformable models and fuzzy affinity," in Information Processing in Medical Imaging.. New York: Springer, 1997, pp. 113–126.
[12] Y. Zhou and J. Bai, "Multiple abdominal organ segmentation: An atlas-based fuzzy connectedness approach," IEEE Trans. Inf. Technol. Biomed., vol. 11, no. 3, pp. 348–352, May 2007.
[13] T. F. Cootes, A. Hill, C. J. Taylor, and J. Haslam, "Use of active shape models for locating structures in medical images," Image Vis. Comput., vol. 12, no. 6, pp. 355–365, 1994.
[14] T. Kitasaka, K. Mori, J.-I. Hasegawa, and J.-I. Toriwaki, "Lung area extraction from 3-D chest X-ray CT images using a shape model generated by a variable Bézier surface," Syst. Comput. Jpn., vol. 34, no. 4, pp. 60–71, 2003.
[15] J. Pu, J. Roos, C. A. Yi, S. Napel, G. D. Rubin, and D. S. Paik, "Adaptive border marching algorithm: Automatic lung segmentation on chest CT images," Comput. Medi. Imag. Graph., vol. 32, no. 6, pp. 452–462, 2008.
[16] U. Bagci, X. Chen, and J. K. Udupa, "Hierarchical scale-based multi object recognition of 3-D anatomical structures," IEEE Trans. Med. Imag., vol. 31, no. 3, pp. 777–789, Mar. 2012.
[17] X. Chen, J. K. Udupa, U. Bagci, Y. Zhuge, and J. Yao, "Medical image segmentation by combining graph cut and oriented active appearance models," IEEE Trans. Image Process., vol. 21, no. 4, pp. 2035–2046,
Apr. 2012.
[18] X. Chen and U. Bagci, "3-D automatic anatomy segmentation based on iterative graph-cut-ASM," Med. Phys., vol. 38, no. 8, pp. 4610–4622, 2011.
[19] B. Li, G. E. Christensen, E. A. Hoffman, G.McLennan, and J.M. Reinhardt, "Establishing a normative atlas of the human lung: Inter subject warping and registration of volumetric CT images," Acad. Radiol., vol. 10, no. 3, pp. 255–265, 2003.
[20] L. Zhang and J. Reinhardt, "3-D pulmonary CT image registration with a standard lung atlas," in Proc. SPIE Conf.Med. Imag., 2000, vol. 4322, pp. 67–77.
[21] L. Zhang, E. A. Hoffman, and J. M. Reinhardt, "Atlas-driven lung lobe segmentation in volumetric X-ray CT images," IEEE Trans. Med. Imag., vol. 25, no. 1, pp. 1–16, Jan. 2006.

ISSN (Print) : 2320 – 3765
ISSN (Online): 2278 – 8875

International Journal of Advanced Research in Electrical, Electronics and Instrumentation Engineering

(An ISO 3297: 2007 Certified Organization)

Vol. 5, Issue 4, April 2016

[22] H. Park, P. H. Bland, and C. R. Meyer, "Construction of an abdominal probabilistic atlas and its application in segmentation," IEEE Trans. Med. Imag., vol. 22, no. 4, pp. 483–492, Apr. 2003.
[23] T. Greitz, C. Bohm, S. Holte, and L. Eriksson, "A computerized brain atlas: Construction, anatomical content, and some applications," J. Comput. Assist. Tomogr., vol. 15, no. 1, pp. 26–38, 1991.
[24] Y. Xu, M. Sonka, G. McLennan, J. Guo, and E. A. Hoffman, "MDCTbased 3-D texture classification of emphysema and early smoking related lung pathologies," IEEE Trans. Med. Imag., vol. 25, no. 4, pp.
464–475, Apr. 2006.
[25] M. J. Gangeh, L. Sørensen, S. B. Shaker, M. S. Kamel, M. De Bruijne, and M. Loog, "A texton-based approach for the classification of lung parenchyma in CT images," in Medical Image Computing and Computer- Assisted Intervention—MICCAI 2010. New York: Springer, 2010, pp. 595–602.